Interaction with tumor-associated macrophages promotes PRL-3-induced invasion of colorectal cancer cells via MAPK pathway-induced EMT and NF-κB signaling-induced angiogenesis

TAO ZHANG*, LU LIU*, WEI LAI, YUJIE ZENG, HEYANG XU, QIUSHENG LAN, PENGWEI SU and ZHONGHUA CHU

Department of Gastrointestinal Surgery, Sun Yat-Sen Memorial Hospital, Sun Yat-Sen University, Guangzhou, Guangdong 510120, P.R. China

Received July 2, 2018; Accepted February 21, 2019

DOI: 10.3892/or.2019.7049

Abstract. Protein phosphatase of regenerating liver-3 (PRL-3) is considered to be metastasis-associated phosphatase and is associated with a poor prognosis. Additionally, tumor-associated macrophages (TAMs) participate in cancer progression. A previous study demonstrated that PRL-3 promotes invasion and metastasis by inducing TAM infiltration. However, the underlying mechanism has not been elucidated. In the present study, western blot analysis, polymerase chain reaction, immunohistochemistry, ELISA, mouse model experiments and functional experiments were performed to confirm that the interaction between TAMs and colorectal cancer (CRC) cells induced epithelial-mesenchymal transition (EMT)-associated features in CRC cells by activating mitogen-activated protein kinase (MAPK) pathways in TAMs and upregulating the expression of interleukin (IL)-6 and IL-8. The neutralization of IL-6 and IL-8 reduced EMT and the invasive and migratory abilities of CRC cells. Therefore, IL-6 and IL-8 were considered important factors in EMT, and in CRC invasion and metastasis. In addition, increased angiogenesis was observed after TAMs were co-cultured with CRC cells that overexpress PRL-3. Vascular endothelial growth factor-A was significantly upregulated, and the nuclear factor-κB (NF-κB) signaling pathway was activated in CRC cells after co-culture. Moreover, nude mice injected with CRC cells with high PRL-3 expression levels tended to generate larger xenografts. Immunohistochemistry results from xenografted CRC cells overexpressing PRL-3 also confirmed the activation of MAPK pathways in xenografts. Overall, the findings indicate that PRL-3 promotes CRC cell invasion and metastasis by activating MAPK pathways in TAMs to initiate the EMT, and PRL-3 promotes angiogenesis by activating the NF-κB pathway in CRC cells.

Correspondence to: Professor Zhonghua Chu, Department of Gastrointestinal Surgery, Sun Yat-Sen Memorial Hospital, Sun Yat-Sen University, 107 Yan Jiang West Road, Guangzhou, Guangdong 510120, P.R. China
E-mail: chu9009@163.com

*Contributed equally

Key words: phosphatase of regenerating liver-3, colorectal cancer, tumor-associated macrophages

Introduction

Colorectal cancer (CRC) is one of the most common causes of cancer-associated mortality worldwide (1,2). Multiple clinical studies have reported that patients with CRC with distant metastases (>50% of patients with HCC have metastasis in the liver), have a poor prognosis, but the underlying molecular mechanisms have not been fully elucidated (3-5). In addition, phosphatase of regenerating liver-3 (PRL-3), a member of the family of protein tyrosine phosphatases, is highly expressed in ~90% of liver metastases of CRC, whereas it is moderately expressed in primary lesions (4). In addition, primary solid tumors with high PRL-3 expression are prone to metastasize to distant tissues (6-9). Many studies have described PRL-3 as a biomarker of a poor prognosis and shorter survival durations.

Recent studies have suggested that inflammatory cells and cytokines present in tumors have a critical role in tumor progression (10). This inflammatory microenvironment is now considered to strongly contribute to tumor metastasis by providing a better environment for tumor cells to grow. Furthermore, evidence had demonstrated that inflammation promotes processes by which cells switch from epithelial phenotypes to mesenchymal phenotypes (epithelial-mesenchymal transition; EMT), which increases invasiveness and the chance of metastasis (2,11,12). In addition, our previous research demonstrated that PRL-3 increases the expression of the chemokine ligand 26 (CCL26), which induces infiltration of tumor-associated macrophages (TAMs), thus enhancing invasion by increasing the expression of interleukin (IL)-6 and IL-8 (4). Elevated levels of serum IL-6 are associated with an

increase in tumor size, the occurrence of liver metastases and a poor prognosis. It has also been reported that IL-8 is involved in EMT in breast cancer (13). However, the underlying mechanisms leading to the increased expression of IL-6 and IL-8, and how these cytokines affect invasion and metastasis in CRC remain unknown.

Angiogenesis is another key element in cancer progression and metastasis (5). EMT provides cancer cells with the ability to survive in the circulatory system and then become established in a distant location (2). However, blood vessels are essential for supplying nutrients to new metastases, to maintain the cells and enable further growth. It was previous reported that PRL-3 participates in invasion, migration, metastasis and angiogenesis (4,8). However, the potential role of TAMs in the process of angiogenesis is not yet clear.

In the present study, it was aimed to determine how the interaction of CRC cells and TAMs functions during the processes of metastasis and angiogenesis in CRC.

Materials and methods

Reagents and antibodies. Fetal bovine serum (FBS) was purchased from Biological Industries (Kibbutz Beit Haemek, Israel); phorbol ester (PMA) was obtained from Sigma-Aldrich (Merck KGaA, Darmstadt, Germany). Radioimmunoprecipitation assay (RIPA) buffer was purchased from Thermo Fisher Scientific, Inc. (Waltham, MA, USA), and RPMI and Dulbecco's modified Eagle's medium (DMEM) media were purchased from Gibco (Thermo Fisher Scientific, Inc.). TRIzol and Prime Script reverse transcription (RT) reagents were purchased from Takara Bio, Inc. (Otsu, Japan), and recombinant CCL26 (rCCL26) was obtained from PeproTech, Inc. (Rocky Hill, NJ, USA). Matrigel matrix was purchased from BD Biosciences (Becton, Dickinson and Company, Franklin, Lakes, NJ, USA). Anti-extracellular signal-regulated 1/2 [ERK(1/2); cat. no. AF0155], anti-phosphorylated (p)-ERK(1/2) (cat. no. AF1015), anti-c-Jun N-terminal kinase (JNK; cat. no. AF6318), anti-IL-8 (cat. no. DF6998), anti-Lamin B (cat. no. BF1002), horseradish peroxidase (HRP)-labeled goat anti-mouse IgG (cat. no. S0002), HRP-labeled goat anti-rabbit IgG (cat. no. S0001) and anti-phosphorylated (p)-JNK antibodies (cat. no. AF3318) were purchased from Affinity Biosciences (Cincinnati, OH, USA). Anti-IL-6 (cat. no. 12153), anti-E-cadherin (cat. no. 3195), anti-Snail (cat. no. 3879), anti-Vimentin (cat. no. 5741), anti-CD68 (cat. no. 79594), anti-NF-κB inhibitor α (IκBα; cat. no. 4812), anti-inhibitor of nuclear factor-κB kinase subunit α (IKKα; cat. no. 61294), anti-P50 (cat. no. 3035) and anti-GAPDH antibodies (cat. no. 5174) were purchased from Cell Signaling Technology, Inc. (Danvers, MA, USA). Anti-CD206 (cat. no. AF2534-SP) was purchase from R&D Systems, Inc. (Minneapolis, MN, USA). Inhibitors of p-JNK (SP600125) and p-ERK (SCH772984) were purchased from MedChemExpress USA (Monmouth Junction, NJ, USA), and IL-6 and IL-8 were purchased from ProteinTech Group, Inc. (Chicago, IL, USA).

Cell cultures and treatments. LoVo, HT29 and THP-1 cells were purchased from the Shanghai Cell Bank of the Chinese Academy of Sciences (Shanghai, China). The cell lines were authenticated in July 2017 by Guangzhou Cellcook Biotech Co., Ltd. (Guangzhou, China), with their STR profiles compared to those in the American type Culture Collection and DSMZ (Braunschweig, Germany) databases. LoVo and THP-1 lines were cultured in RPMI-1640 medium, while HT29 cells were cultured in in DMEM; all cells were supplemented with 10% FBS, 100 mg/ml streptomycin and 100 mg/ml penicillin. Western blot analysis was performed to identify PRL-3 expression in these CRC cell lines, and the results showed that HT29 cells expressed high levels of PRL-3, while LoVo cells expressed low levels. Therefore, LoVo cells were selected for constructing PRL-3-overexpression lines, and HT29 cells were chosen for the knockdown groups. Stable transfection of pAcGFP negative control (LoVo-NC) and pAcGFP-PRL-3 (LoVo-P) vectors from Shanghai GeneChem (Shanghai, China) was performed, resulting in control vector-transfected and PRL-3-overexpression cell lines, respectively. To knock down PRL-3, HT29 cells were stably transfected with PRL-3 short hairpin RNA (shRNA; HT29-P), and an shRNA control was used in negative control groups (Fig. S1). The sequence of shRNA-PRL-3 was as follows: 5'-ACAGAGGCTGCG GTTCAAA-3'. The sequence of negative control was: 5'-TTC TCCGAACGTGTCACGT-3'. THP-1 cells were transformed into M1 and M2 macrophages as previously described (4,14). THP-1 cells differentiated into M2 macrophages after treatment with PMA for 6 h and IL-4 for 18 h (a total of 24 h). The cells mentioned above were incubated at 37˚C in a humidified 5% CO_2 atmosphere. Subsequent experiments were performed in >24 h after the transfection.

Western blot assay. Cells were washed with phosphate-buffered saline (PBS) and then lysed on ice with RIPA buffer [50 mM Tris, 150 mM NaCl, 1% NP-40, 0.5% sodium deoxycholate, 0.1% SDS, 2 mM EDTA (pH 7.5)] containing 1% cocktail and 1% phosphatase inhibitor. Protein concentration was determined by the Bradford protein assay using bovine serum albumin (BSA) as a standard. Equal amounts of proteins (30 μg/lane) were separated by SDS-PAGE with 10 or 12% polyacrylamide gels. Proteins separated in the gels were transferred to PVDF membranes and then blocked in 5% BSA at room temperature for 90 min. After blocking, the membranes were washed three times with Tris-buffered saline + 0.1% Tween-20, incubated overnight at 4˚C with the relevant primary antibodies, washed again and incubated with goat anti-rabbit IgG (1:8,000) or goat anti-mouse IgG conjugated with HRP (1:8,000) for 1 h at room temperature. The dilution of each primary antibody was as follows: E-cadherin, Snail, Vimentin, VEGF-A, IL-6 and IL-8 were 1:600; GAPDH and Lamin B were 1:1,000; ERK(1/2), p-ERK(1/2), JNK and p-JNK are 1:500; IκBα, p-IκBα, IKKα and p-IKKα were 1:1000; P50 was 1:800. Labeled proteins were visualized and measured using chemiluminescence (eECL Western Blot Kit, Beijing ComWin Biotech Co., Ltd., Beijing, China).

Co-culture of TAMs (M2 macrophages) with CRC cells. M2 macrophages (a total of $5x10^5$) were transformed and seeded onto 6-well plates, with HT29-NC, HT29-P, LoVo-P and LoVo-NC cells ($2x10^6$ each) co-cultured in upper Transwell inserts for 48 h. The ratio of M2 cells to tumor cells was 1:4. After co-culturing for 24 h, the cells were washed, and the

cell culture supernatant was collected for further experiments. Flow cytometry was used to confirm M2 cells by identifying CD68 and CD206 as markers.

Cell invasion, migration and wound-healing assays. Transwell inserts were applied to detect cell invasion. LoVo-P, LoVo-NC, HT29-NC or HT29-P cells ($8x10^4$ each) were diluted in 0.2 ml of serum-free RPMI-1640 medium and added to the upper chamber that had 10% Matrigel on the surface, with M2 macrophages ($5x10^5$) seeded in the lower chamber. Before combining the chambers, JNK/ERK inhibitors, anti-IL-6 or anti-IL-8 were added to the M2 macrophage culture for 2 h; then, the medium was replaced with RPMI-1640 medium. The cells were incubated at 37˚C in a humidified atmosphere containing 5% CO_2. After 24 h, invasive CRC cells located on the lower side of the chamber were fixed with 4% paraformaldehyde for 25 min at room temperature, stained with 0.1% crystal violet in methanol for 15 min at room temperature, air dried, screened and counted under a microscope. Similarly, LoVo-P and LoVo-NC ($1x10^6$) were seeded in 6-well plates and cultured overnight. The cells were divided into three groups. Two of the groups were exposed to inhibitors of p-JNK (SP600125; 2.5 and 5 nM) and p-ERK (SCH772984; 4 and 8 nM) for 2 h, while the third served as the negative control. Cell migration was measured by determining the movement of cells into a scraped area created by the tip of a 200-μl pipette. The degree of 'wound closure' was examined after 24 and 48 h. After cell adherence, the remaining gap was then assessed using light microscopy and quantified using ImageJ (National Institutes of Health, Bethesda, MA, USA; ImageJ bundled with 64-bit Java 1.8.0_112).

ELISA. IL-6, IL-8 and vascular endothelial growth factor-A (VEGF-A) were assayed in the culture supernatants from the tested cells using a Quantikine Kit (cat. no. CSB-E04638h for IL-6; cat. no. CSB-E04641h for IL-8; CUSABIO Technology LLC, Houston, TX, USA) according to the manufacturer's protocol. The specific cells and the various conditions applied to these cells are listed in the Results.

Immunohistochemistry (IHC) assay. IHC was performed to detect p-JNK, and p-ERK using an Ultra-Sensitive SP IHC Kit (cat. no. KIT-9710; Fuzhou Maixin Biotech Co., Ltd., Fuzhou, China) according to the manufacturer's instructions. Normal IgG was used as a negative control. Images were captured with a Zeiss laser-scanning microscope (Carl Zeiss AG, Oberkochen, Germany) with a core data acquisition system (NIS elements 4.0; Nikon Corporation, Tokyo, Japan).

Human angiogenesis array analysis. The RayBio Human Angiogenesis Array G1000 (RayBiotech Life, Norcross, GA, USA), which consists of 43 different human angiogenesis-associated antibodies spotted on a membrane, was used in the present study according to the manufacturer's instructions. The membranes were blocked in blocking buffer at 37˚C for 30 min and incubated with protein samples at 37˚C for 1 h. After washing, the membranes were incubated with diluted biotin-conjugated antibodies at 37˚C for 2 h. After the membranes were washed again, HRP-conjugated streptavidin (1:1,000 dilution) was added and incubated for 2 h. Membranes were then washed thoroughly and exposed to detection buffer in the dark. By comparing the signal intensities, relative expression levels of proteins were determined. Signal intensities were quantified by densitometry (ImageJ; National Institutes of Health; ImageJ bundled with 64-bit Java 1.8.0_112).

Mouse tumor model. Athymic nude mice (BALB/c nude, 6-week-old males) were purchased from the Laboratory Animal Science Center of Guangdong Province (Guangzhou, China) and maintained under defined conditions (12-h light cycle in a room maintained at 21±1˚C and 50±10% humidity) at the Animal Experiment Center of Sun Yat-Sen University. Food was provided at the same time each day with *ad libitum* access to water in the cage. All animal protocols were approved by the Institutional Animal Care and Use Committee and Welfare Committee of Sun Yat-Sen University (Guangzhou, China). These mice were divided into four groups, with six mice randomly chosen for each group. Mice in each group were injected with LoVo-NC, LoVo-P, HT29-NC or HT29-P cells at $5x10^6$ cells each into the subcutaneous tissue of the left flank. After injection, the mice were maintained in pathogen-free environments. All mice were sacrificed on day 30, and the xenografted tumors were excised from the animals for further study, including IsHC assays. The formula we used to calculate the volume of xenograft was as follows: Volume = [major axis x $(\text{minor axis})^2$]/2.

Statistical analysis. Statistical analysis was performed using SPSS 22.0 (IBM Corp., Armonk, NY, USA). All data obtained from each experiment are presented as the mean ± standard deviation of three separate experiments. A post hoc test (Bonferroni) was used following one-way analysis of variance (ANOVA) for statistical analysis. The differences between two groups and among three or more groups were determined using Student t-tests and one-way ANOVAs, respectively. All experiments were performed independently. $P<0.05$ was considered to indicate a statistically significant difference.

Results

Co-culture of TAMs and CRC cells with high PRL-3 expression promotes EMT. EMT is believed to have a critical role in cancer metastasis, during which cancer cells tend to become a more invasive and develop a metastatic phenotype. In addition, the extent of EMT can be characterized by detecting several proteins, including E-cadherin, Snail and Vimentin, via western blot analysis. To explore the effect of co-culturing, LoVo-P or HT29 cells, both with high PRL-3 expression levels, and TAMs were used in a co-culture system. After 24 h of co-culture, EMT markers in CRC cells, including E-cadherin, Snail and Vimentin expression in LoVo-P and HT29 cells, were significantly altered (Fig. 1). Co-culturing CRC cells and TAMs downregulated the expression of E-cadherin, and upregulated the expression of Snail and Vimentin, which suggested that CRC cells acquired a mesenchymal phenotype when co-cultured with TAMs.

PRL-3-induced activation of IL-6 and IL-8 is based on the MAPK pathway in TAMs. Our previous study suggested that PRL-3 promoted CRC cell invasion by initiating signaling

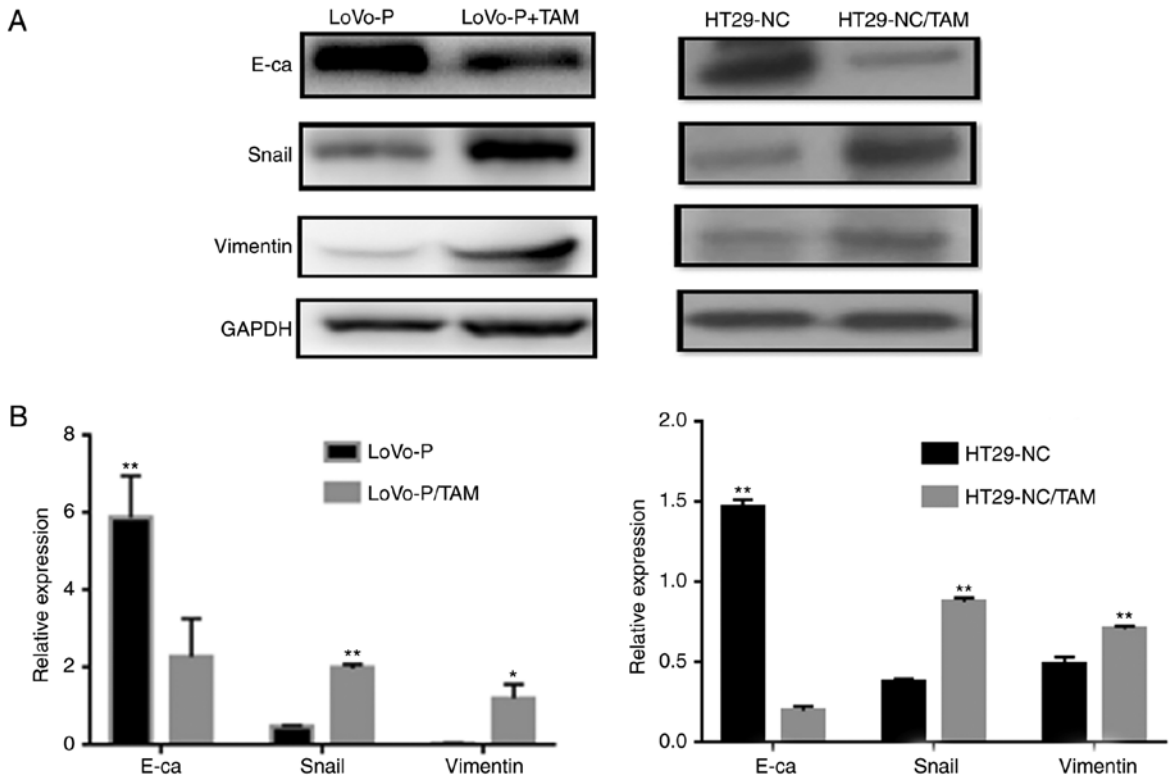

Figure 1. Co-culture of TAMs and LoVo-P or HT29-NC cells promotes EMT. (A) Expression of EMT-associated proteins in LoVo-P and HT29 cells after coculture with TAMs and (B) densitometry analysis. *P<0.05, **P<0.01. EMT, epithelial-mesenchymal transition; LoVo-P, PRL-3 overexpression; TAM, tumor-associated macrophages; NC, negative control; E-ca, E-cadherin.

pathways in TAMs (4). To explore the molecular mechanism underlying PRL-3-induced IL-6 and IL-8 production, western blot assays were performed to elucidate the phosphorylation status of proteins that may be involved after the co-culture of CRC cells (LoVo-P, LoVo-NC, HT29-NC and HT29-P) and TAMs, such as the phosphorylated forms of JNK and ERK. PRL-3 induced the phosphorylation of JNK and ERK in TAMs. MAPK pathway activation was suppressed after downregulating PRL-3 (Fig. 2A). Additionally, IL-6 and IL-8 levels were changed by silencing/overexpression of PRL-3 levels.

To examine whether the MAPK/JNK pathway or the MAPK/ERK pathway regulated IL-6 and IL-8 production, inhibitors of p-JNK (SP600125, 2.5 and 5 nM) and p-ERK (SCH772984, 4 and 8 nM) were added to the TAM cultures prior to co-culture with CRC cells. The western blot analysis illustrated that both p-JNK and p-ERK were suppressed as the inhibitor concentration increased (Fig. 2B and C). Similarly, IL-6 and IL-8 levels declined significantly when the MAPK signaling pathways were suppressed. Additionally, ELISAs were performed to identify the extracellular levels of IL-6 and IL-8, which confirmed the results of the western blot assays. The results showed that the PRL-3-induced IL-6 and IL-8 expression was abolished by the addition of JNK and ERK inhibitors, resulting in the downregulation of IL-6 and IL-8 (Fig. 3A and B). Additionally, cell invasion assays were performed to examine whether invasiveness was regulated by MAPK pathways. The invasive and metastatic capacities of HT29-NC and LoVo-P cells were reduced by blocking JNK and ERK signaling. As the concentrations of inhibitors increased, the number of cells invading through the membrane down from the upper chamber gradually declined (Fig. 3C and D).

PRL-3 and activated MAPK pathways in TAMs. Our previous study demonstrated that PRL-3 in CRC cells upregulated the expression of CCL26, which induced TAM infiltration, enhancing the invasiveness of CRC cells (4). As it was found that PRL-3 was involved in the initiation of MAPK pathways, the potential association between CCL26 and MAPK signaling was examined. CCL26 was added to the lower chamber of the co-culture system with CRC cells (HT29-P, PRL-3 shRNA knockdown) and TAMs to detect the phosphorylation of JNK and ERK, and the expression of IL-6 and IL-8 in TAMs via western blot analysis. ELISAs were used to identify the extracellular levels of IL-6 and IL-8 after collecting the cell culture supernatant. In addition, cell invasion assays were performed to clarify whether CCL26 increased the invasiveness of HT29-P cells. The analysis showed that JNK and ERK signaling in TAMs were both triggered by the addition of CCL26 (10 and 100 ng/ml) even when PRL-3 expression in HT29 cells was suppressed (Fig. 4A and B). Furthermore, analysis of the lower Transwell chamber containing CCL26 (100 ng/ml) showed that the migratory activity of HT29-P cells was more pronounced than that of those without CCL26 after 24 h in co-culture (Fig. 4C and D). Meanwhile, the levels of IL-6 and IL-8 in co-cultured TAMs, both intracellular and extracellular, were upregulated compared with those in cells not treated with CCL26 (Fig. 4E and F).

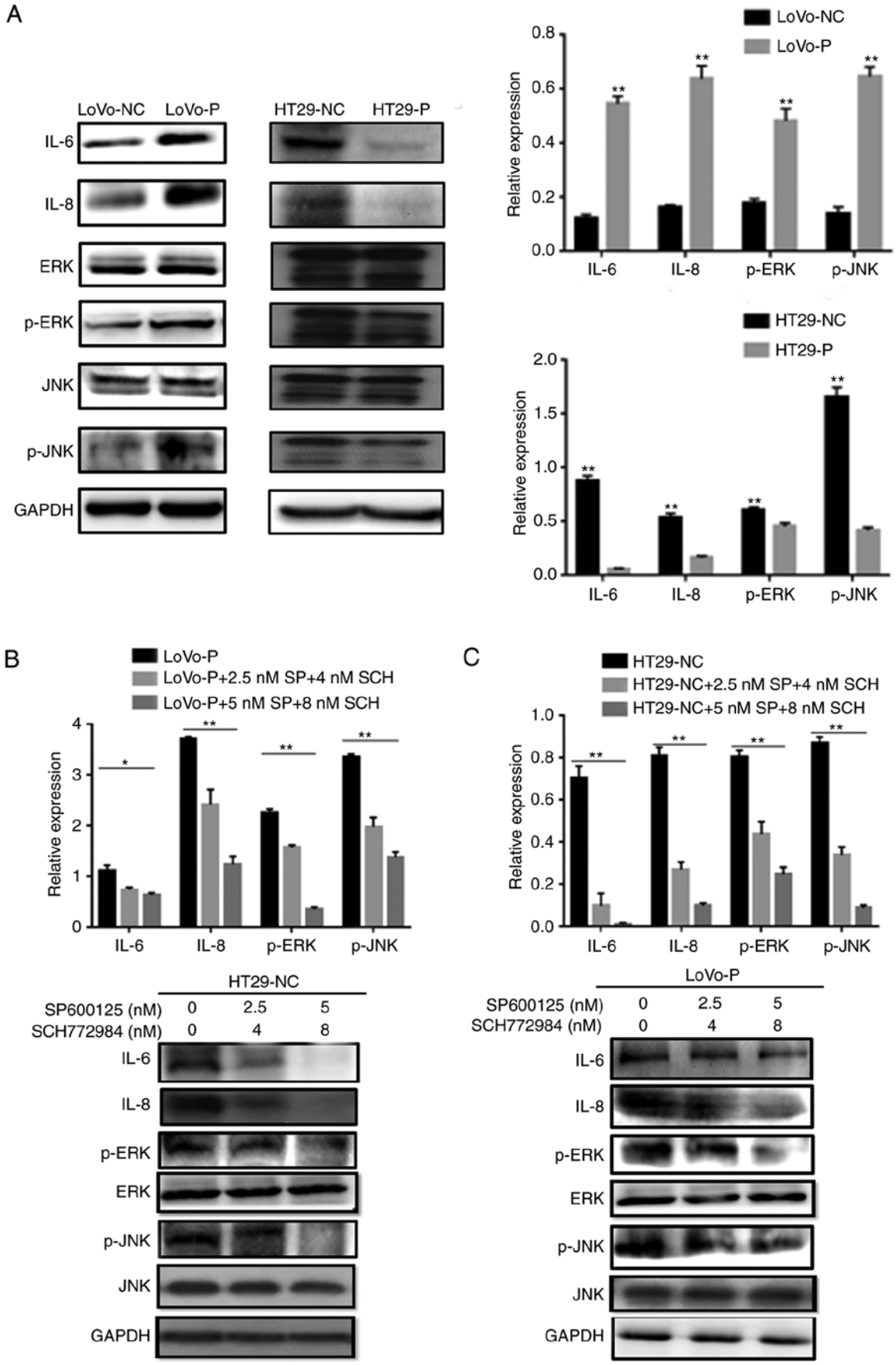

Figure 2. PRL-3-induced activation of IL-6 and IL-8 by initiating JNK and ERK pathways in TAMs. (A) After co-culture with colorectal cancer cells, IL-6, IL-8, p-JNK, and p-ERK levels in TAMs were examined using western blot assays. In (B) LoVo-P and (C) HT29-NC cells, IL-6 and IL-8 expression was detected after the addition of an inhibitor to p-JNK (SP600125; 2.5 and 5 nM) or p-ERK (SCH772984; 4 and 8 nM) into the co-culture system with LoVo-P cells. *P<0.05, **P<0.01. PRL-3, phosphatase of regenerating liver-3; NC, negative control; LoVo-P, LoVo PRL-3 overexpression; HT29-P, HT29 PRL-3 knockdown; IL, interleukin; ERK, extracellular signal-regulated kinase; p, phosphor; JNK, c-Jun N-terminal kinase; SP, SP600125; SCH, SCH772984.

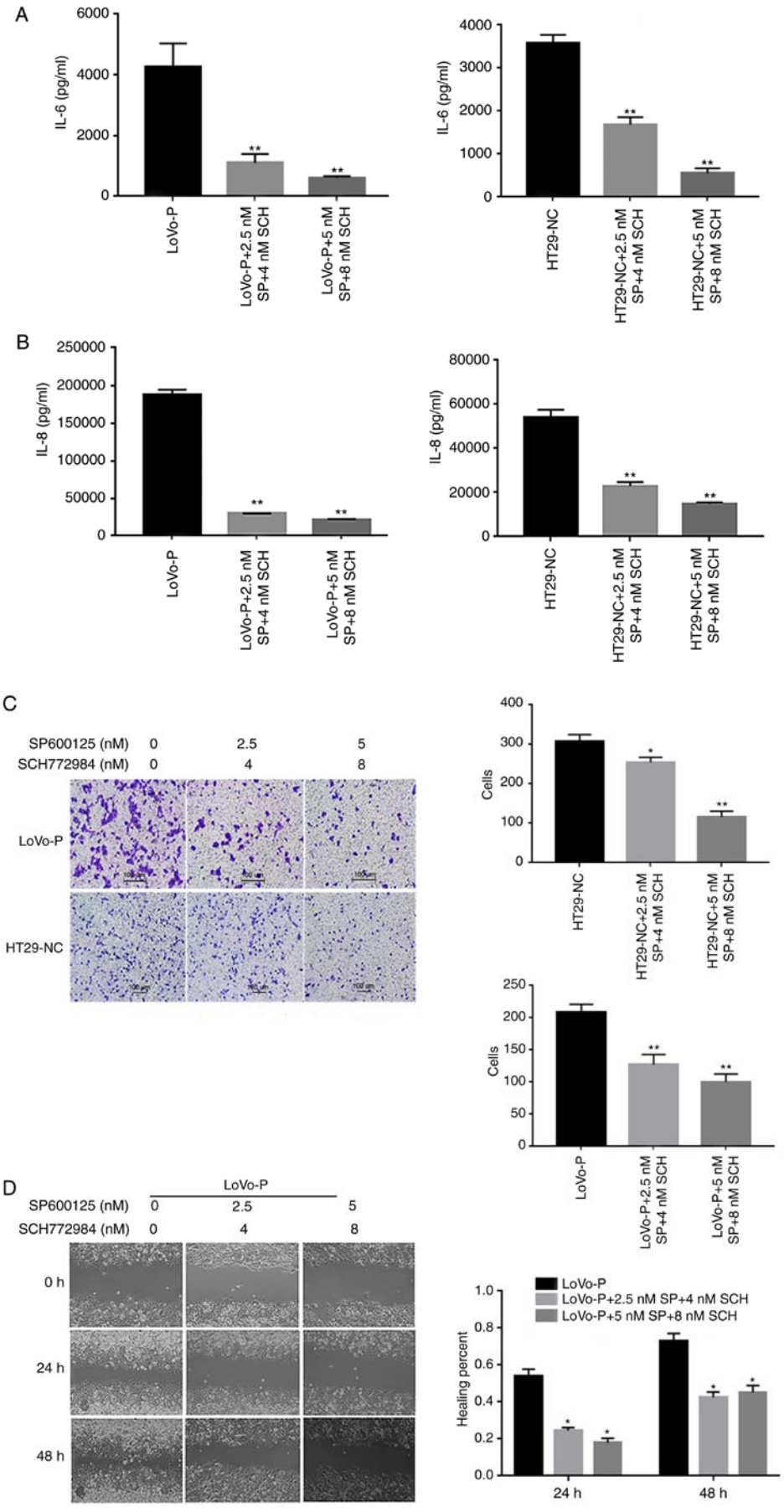

Figure 3. MAPK pathway regulates invasion of CRCs. (A) IL-6 and (B) IL-8 expression in supernatants from co-culture systems measured by ELISA. (C) Blocking ERK and JNK decreases the invasiveness of colorectal cancer cells. (D) A wound-healing assay showed the same trend. *P<0.05, **P<0.01 vs. respective control. PRL-3, phosphatase of regenerating liver-3; ERK, extracellular signal-regulated kinase; p, phosphor; JNK, c-Jun N-terminal kinase; LoVo-P, LoVo PRL-3 overexpression; NC, negative control; SP, SP600125; SCH, SCH772984; IL, interleukin.

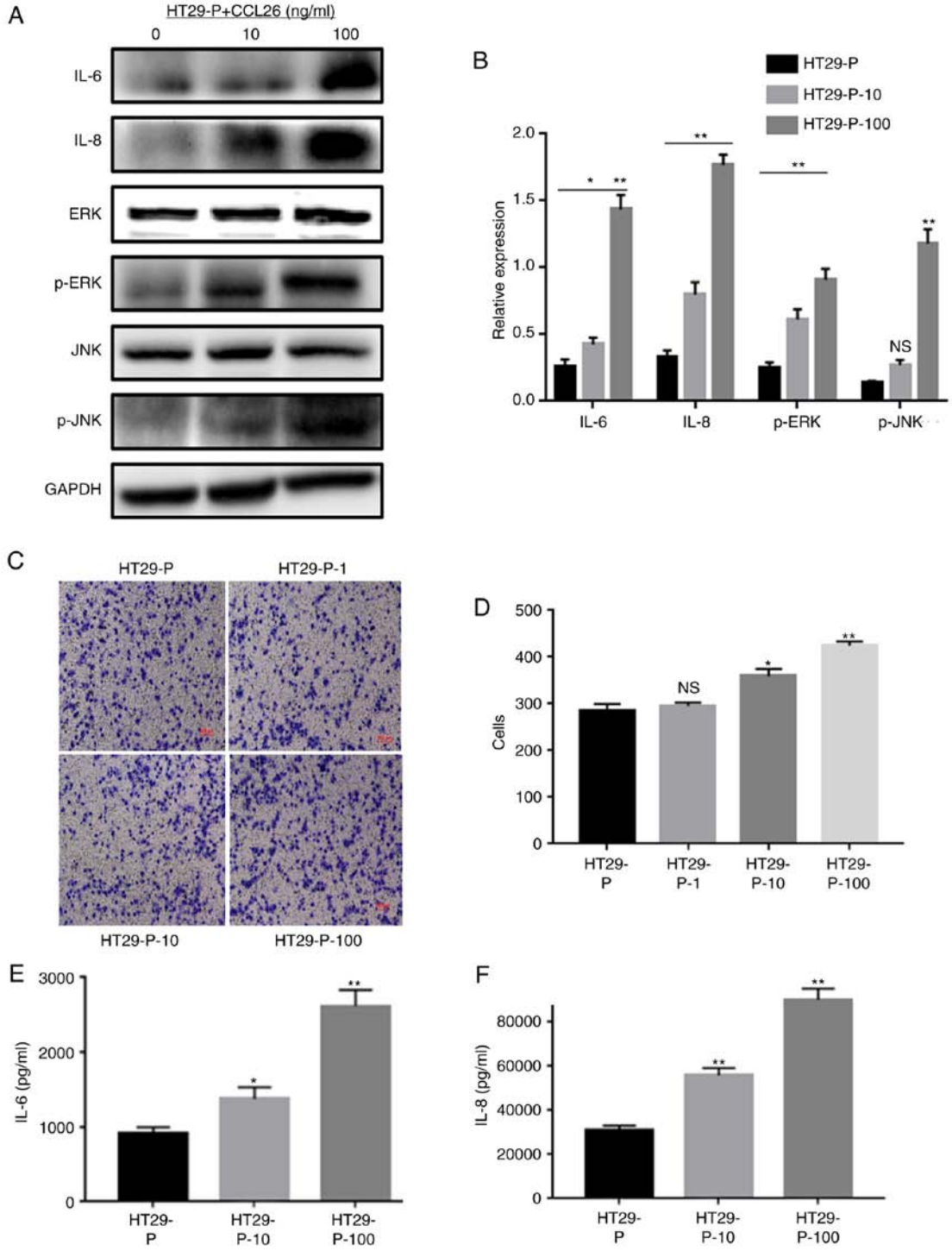

Figure 4. CCL26 increases the expression of IL-6 and IL-8 and the activation of p-JNK and p-ERK in HT29-P cells, resulting in an increase in the invasiveness of CRC cells. (A) Western blot assays and (B) densitometry analysis were performed to measure the expression of IL-6, IL-8, p-JNK, and p-ERK. (C and D) Invasion and migration were analyzed in Matrigel invasion assays. (E) IL-6 and (F) IL-8 were determined by ELISA. *P<0.05, **P<0.01, NS, not significant. PRL-3, phosphatase of regenerating liver-3; HT29-P, HT29 PRL-3 knockdown; CCL26, chemokine ligand 26; IL, interleukin; ERK, extracellular signal-regulated kinase; p, phosphor; JNK, c-Jun N-terminal kinase; 10, 10 ng/ml CCL26; 100, 100 ng/ml CCL26; 1, 1 ng/ml CCL26.

IL-6 and IL-8 induced EMT in CRC cells. To further determine the role of IL-6 and IL-8 in EMT in CRC, the protein levels of E-cadherin, Snail and Vimentin were analyzed in LoVo-NC, LoVo-P, HT29-NC and HT29-P cells after 24 h of co-culture with TAMs. LoVo-P and HT29-NC cells expressed higher levels of IL-6 and IL-8 than LoVo-NC and HT29-P cells, respectively (Fig. 2A). And after adding inhibitors of JNK (SP600125, 2.5 and 5 nM) and ERK (SCH772984, 4 and 8 nM) into co-culture system, E-cadherin was increased, and Snail and Vimentin were reduced as the concentration of inhibitors increased (Fig. 5A).

Additionally, antibodies against IL-6 and IL-8 were added to the co-culture system, and protein levels in the HT29-NC and LoVo-P cells, in the upper chamber, were detected by

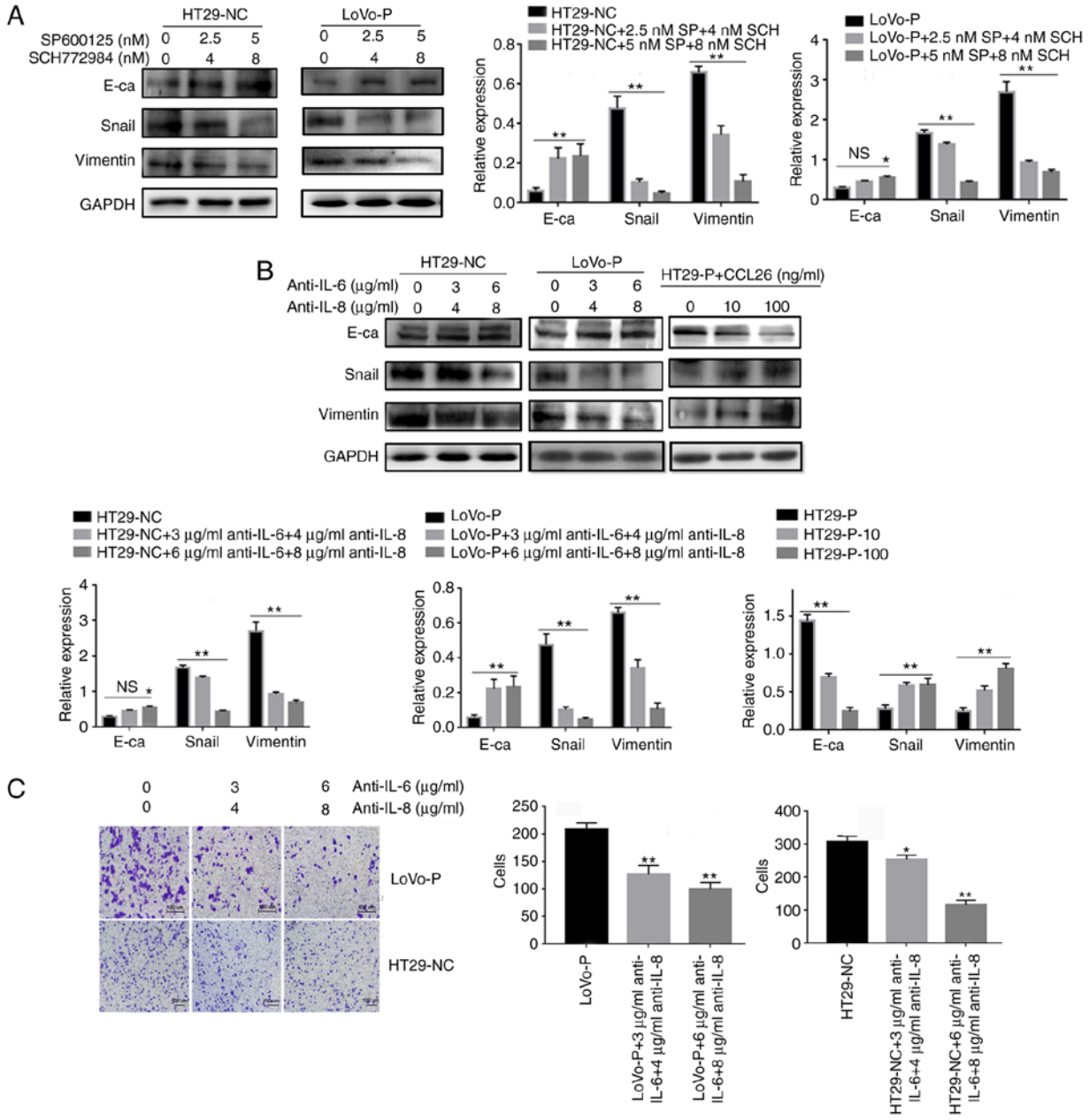

Figure 5. IL-6 and IL-8 induced epithelial-mesenchymal transition in CRC cells, which was regulated by MAPK and PRL-3. (A) After neutralizing the MAPK pathways in TAMs, the levels of E-cadherin, Snail and Vimentin in colorectal cancer cells were examined using western blot assays. (B) IL-6 (3 and 6 μg/ml) and IL-8 (4 and 8 μg/ml) antibodies, and the addition of CCL26, were used and the levels of E-cadherin, Snail and Vimentin in CRC cells were examined using western blot assays. (C) Invasion was evaluated by Matrigel invasion assays after blocking IL-6 (3 and 6 μg/ml) and IL-8 (4 and 8 μg/ml) *P<0.05, **P<0.01 vs. appropriate controls, NS, not significant. PRL-3, phosphatase of regenerating liver-3; MAPK, mitogen-activated protein kinase; NC, negative control; LoVo-P, LoVo PRL-3 overexpression; HT29-P, HT29 PRL-3 knockdown; E-ca, E-cadherin; SP, SP600125; SCH, SCH772984; IL, interleukin; CCL26, chemokine ligand 26.

western blot analysis. The neutralizing antibodies increased the expression of E-cadherin and reduced the expression of Snail and Vimentin in CRC cells (Fig. 5B). Transwell analysis also indicated that CRC cells treated with neutralizing antibodies targeting IL-6 and IL-8 tended to have fewer cells that migrated successfully (Fig. 5C).

PRL-3 promotes angiogenesis by activating the nuclear factor-κB (NF-κB) pathway. After co-culture with TAMs, angiogenesis-associated proteins in the supernatants of LoVo-P and LoVo-NC cells were evaluated using a Human Angiogenesis Array to identify the potential effects. Protein levels of neurotrophin-4, VEGF, VEGF receptor 2 and VEGF-D in LoVo-P cells were at least 2-fold higher than in LoVo-NC cells (Fig. 6A). Then, VEGF-A, which is the major factor in blood vessel formation, was chosen for further examination. RT-qPCR results indicated that VEGF-A expression in LoVo-P cells was upregulated significantly in 3 days of co-culture, while VEGF-A expression in LoVo-NC cells showed no significant differences over the whole experimental period. In addition, supernatants were examined via ELISA assays and found that VEGF-A expression in LoVo-P cells increased to ~2,000 ng/ml after 3 days of co-culture, while in LoVo-NC cells and TAMs, the levels remained steady (Fig. 6B).

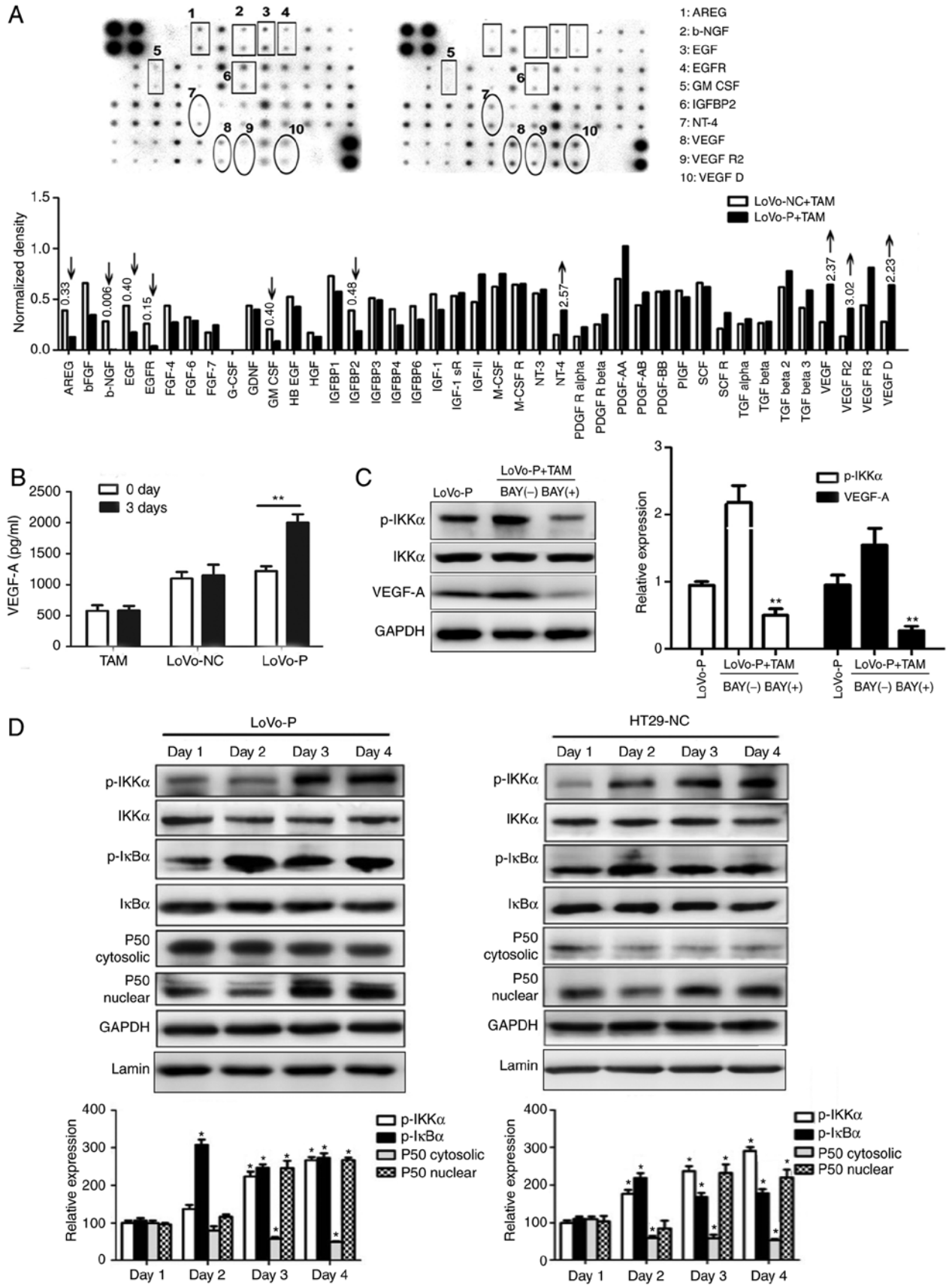

Figure 6. PRL-3 promotes angiogenesis by activating the NF-κB pathway. (A) Angiogenesis-associated proteins in supernatants from LoVo-P and LoVo-NC cells. (B) ELISAs were used to detect VEGF-A in LoVo-P and LoVo-NC cells after co-culture with TAMs. **P<0.01. (C) After suppressing the NF-κB pathway, VEGF-A expression in LoVo-P cells was determined. **P<0.01 vs. BAY(-). (D) NF-κB pathway activation was examined by western blot analysis. *P<0.05. PRL-3, phosphatase of regenerating liver-3; VEGF, vascular endothelial growth factor; TAM, tumor-associated macrophage; NC, negative control; LoVo-P, LoVo PRL-3 overexpression; p, phosphor; IKKα, nuclear factor κ-B kinase subunit α; AREG, amphiregulin; b-NGF, β nerve growth factor; EGF, epidermal growth factor; EGFR, epidermal growth factor receptor; GM-CSF, granulocyte-macrophage colony-stimulating factor; IGFBP2, insulin-like growth factor-binding protein 2; NT-4, neurotrophin-4; VEGFR2, vascular endothelial growth factor receptor 2; IκBα, NF-κB inhibitor α.

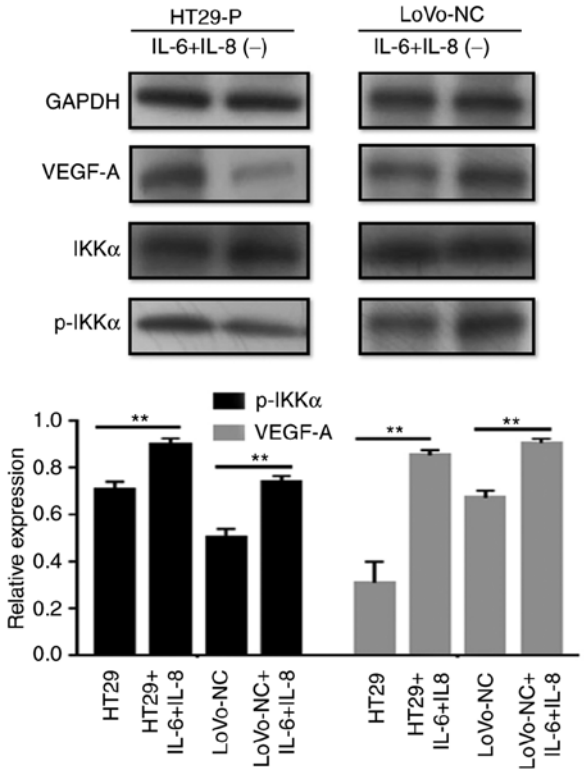

Figure 7. IL-6 and IL-8 activate the NF-κB pathway. With the addition of IL-6 (200 ng/ml) and IL-8 (10 ng/ml) to LoVo-NC and HT29-P, NF-κB pathway activation was detected. p-IKKa relative to IKKa. **P<0.01. PRL-3, phosphatase of regenerating liver-3; HT29-P, HT29 PRL-3 knockdown; NC, negative control; IL, interleukin; p, phosphor; IKKα, nuclear factor κ-B kinase subunit α; VEGF, vascular endothelial growth factor.

NF-κB is a key regulator of innate immunity and inflammation. Jedinak *et al* (15) suggested that NF-κB might be associated with the expression of VEGF. Therefore, it whether the NF-κB pathway was activated in CRC cells was explored by performing western blot analysis (Fig. 6C and D). The levels of the phosphorylated forms of IκBα and IKKα increased, and nuclear P50 showed a similar trend during to co-culture. To determine the association between NF-κB and VEGF-A, an inhibitor of NF-κB (BAY 11-7082) was added to the co-culture system. Consequently, p-IKKα levels were reduced by BAY 11-7082, as was VEGF-A. Additionally, to explore the potential mechanism between the MAPK and NF-κB pathways, IL-6 (200 ng/ml) and IL-8 (10 ng/ml) was added to LoVo-NC and HT29-P co-culture with TAMs to detect NF-κB pathway activation. The result showed that IL-6 and IL-8 activated the NF-κB pathway (Fig. 7).

JNK and ERK activation in CRC xenografts. To investigate the effect of TAM infiltration induced by PRL-3 on tumor growth and angiogenesis *in vivo*, mice were inoculated with equal numbers of LoVo-P, LoVo-NC, HT29-NC and HT29-P cells into the subcutaneous tissue of the left flank of nude mice (Fig. 8). After 30 days, the animals were sacrificed, and the tumor xenografts were excised for further experiments. IHC analyses of were performed using these xenografts to compare the level of p-JNK and p-ERK (Fig. 8A and B). The results showed that the proteins mentioned above were obviously higher in xenografts from LoVo-P and HT29-NC cells than those from LoVo-NC and HT29-P cells, respectively, which suggested that MAPK activation induced by PRL-3 was associated with tumor growth (Fig. 8C). Tumors were larger in groups with high levels in PRL-3 expression from cells (LoVo-P, HT29-NC) than in cells with low PRL-3 (LoVo-NC, HT29-P; Fig. 8C). TAMs were present in the tumor xenografts and showed no obvious difference between groups (Fig. S2).

Discussion

Increasing numbers of studies have emphasized the interaction of the tumor microenvironment and tumor cells in the promotion of tumor progression, angiogenesis and invasion (11,14-17). In addition, TAMs, one of the most investigated cancer-associated factors, have been demonstrated to be associated with cancer prognosis (15-17). Various inflammatory cells and cytokines associated with this process have been investigated (10). Our previous studies found that TAM infiltration plays a critical role in CRC progression, and IL-6 and IL-8 secretion is upregulated when PRL-3 is overexpressed in cancer cells (4,14). Additionally, previous studies have suggested that PRL-3 might be a crucial effector in the MAPK cascade (18). In the present study, the phosphorylation of JNK and ERK in TAMs was increased after co-culture with HT29-NC and LoVo-P cells, both of which overexpressed PRL-3. Additionally, the activation of JNK and ERK was associated with high levels of IL-6 and IL-8. Notably, the two MAPK pathways were blocked with specific inhibitors, IL-6 and IL-8 expression was notably reduced. These results illustrated that PRL-3 activated JNK and ERK signaling pathways in TAMs, resulting in the secretion of IL-6 and IL-8.

In CRC, EMT is associated with an invasive and metastatic phenotype (19). Rokavec *et al* (12) demonstrated that the activation of the IL-6 receptor/STAT3/microRNA-34a loop by IL-6 induces EMT, which promotes invasion and a metastatic cascade. In our experiments, the upregulation of IL-6 and IL-8 was consistent with the downregulation of E-cadherin and the upregulation of Snail and Vimentin. In addition, invasion assays demonstrated that IL-6 and IL-8 are indicators of the number of migrating cells. An opposite trend was produced when JNK and ERK were inhibited, according to the western blot analysis and invasion assay. Furthermore, the migratory ability of CRC cells declined when IL-6 and IL-8 were neutralized by antibodies. All of these results suggested that PRL-3 promoted the invasion of CRC cells by initiating MAPK pathways in TAMs and activating EMT. Our previous experiments found that PRL-3 promoted CCL26 expression in CRC cells, which induced TAM infiltration to establish the tumor microenvironment (4). CCL26 was added to HT29-P cell cultures to determine the potential effects. Even though PRL-3 expression was reduced, the addition of CCL26 still activated JNK and ERK pathways, contributing to EMT. Therefore, CCL26 might be the key factor connecting TAMs and the events that trigger a series of processes associated with tumor progression.

PRL-3 has been reported as a biomarker of an increased risk of metastasis and poor prognosis (20). For example, Sahai and Marshall (21) found that PRL-3 can stimulate Rho

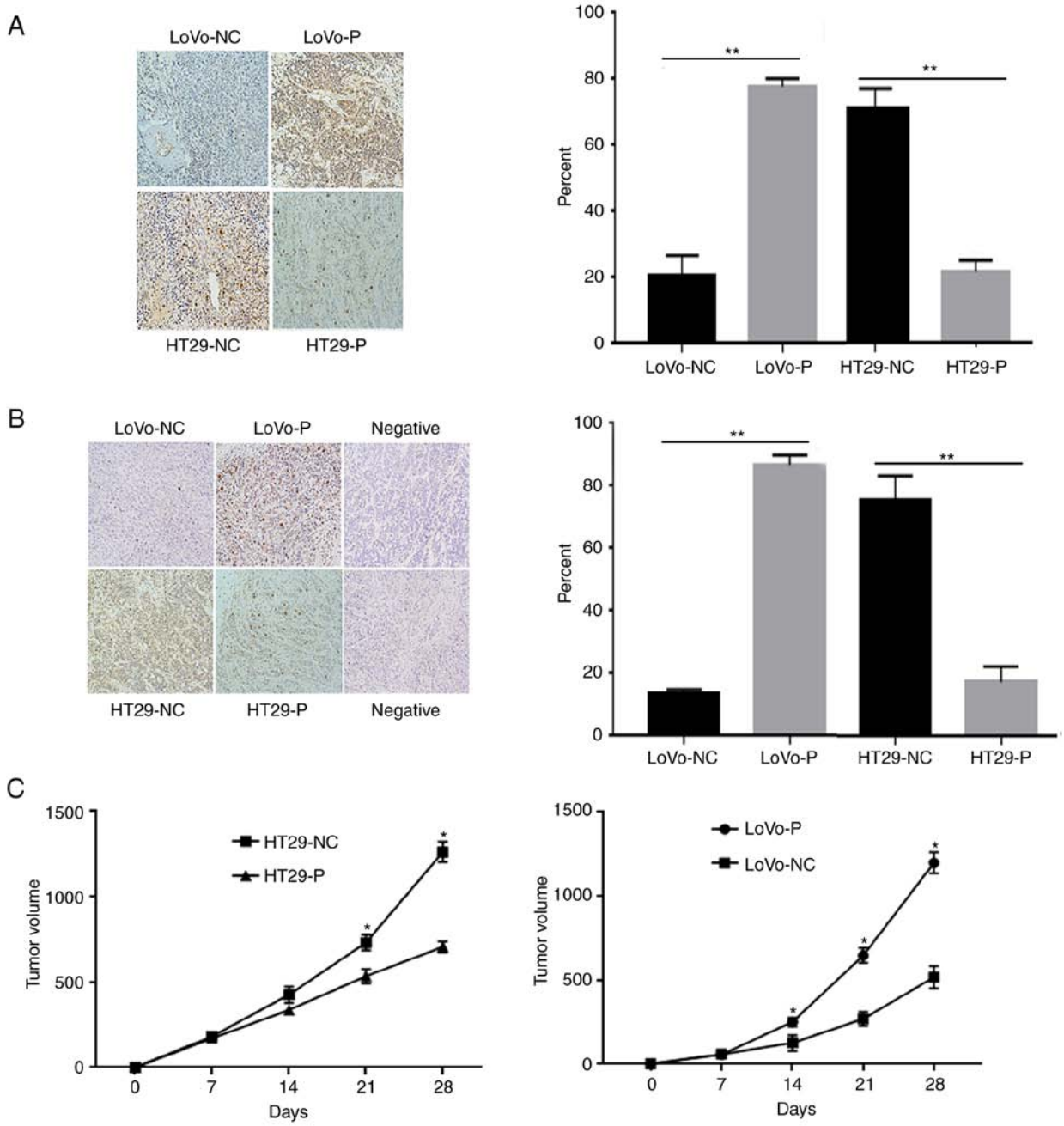

Figure 8. PRL-3 activated JNK and ERK pathways, and promoted tumor growth. Detection of (A) p-JNK and (B) p-ERK in xenografts. The images are obtained under identical microscope and magnification conditions. (C) Xenograft volumes. *P<0.05, **P<0.01 vs. respective control. PRL-3, phosphatase of regenerating liver-3; NC, negative control; LoVo-P, LoVo PRL-3 overexpression; HT29-P, HT29 PRL-3 knockdown.

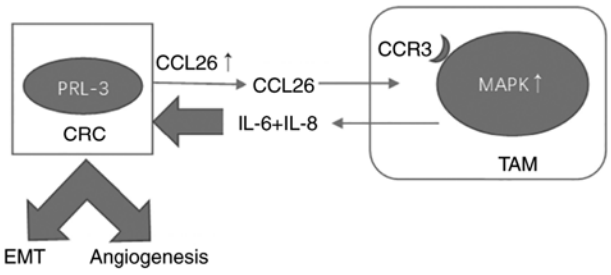

Figure 9. Schema of the mechanism between PRL-3, MAPK and NF-κB. PRL-3, phosphatase of regenerating liver-3; CRC, colorectal cancer; EMT, epithelial-mesenchymal transition; CCL26, chemokine ligand 26; IL, interleukin; CCR3, C-C chemokine receptor type 3; MAPK, mitogen-activated protein kinase; TAM, tumor-associated macrophages.

family GTPase signaling pathways to promote cell motility and invasion. Furthermore, PRL-3 has been suggested to regulate several pathways, such as the PI3K/AKT (22), Src (7) and ERK (6) pathways. In the current experiments, high levels of PRL-3 were with larger xenografts in nude mice. Additionally, p-JNK, p-ERK and VEGF-A expression in cells overexpressing PRL-3 was also upregulated. These results illustrate that PRL-3 has an important role in tumor progression.

The growth of solid tumors is dependent on angiogenesis, which provides the blood supply needed for metastasizing cells to flourish. Various studies have explored the relationship between PRL-3 and angiogenesis. For instance, Guo *et al* (8)

suggested that PRL-3 may be involved in triggering angiogenesis and establishing the tumor microvasculature. Zimmerman *et al* (9) found that PRL-3 is involved in VEGF signaling and blood vessel formation *in vitro* and *in vivo*. In our research, a Human Angiogenesis Array was used and found that VEGF expression was significantly increased in LoVo-P cells compared with that in LoVo-NC cells in co-culture with TAMs. Additionally, a prolonged co-culture resulted in a marked upregulation of VEGF-A expression in LoVo-P cells, while expression in LoVo-NC cells showed no notable difference. Previous research demonstrated that cytokines secreted by TAMs might induce NF-κB activation in CRC cells and VEGF expression. (15). NF-κB is a key regulator of innate immunity and inflammation; the results are consistent with this function. Both in the LoVo and HT29 cell lines, NF-κB activation was enhanced with an increase in co-culturing time, indicating the importance of PRL-3 and the tumor microenvironment in the process of angiogenesis. Furthermore, the addition of IL-6 and IL-8 activated the NF-κB pathway in CRC, which indicated that MAPK signaling is involved in the activation of NF-κB (Fig. 9). There are still some experiments required to fully illustrate the mechanisms of angiogenesis, such as IHC to identify microvessels in the mice xenograft tissues, which would confirm the promotion of angiogenesis *in vivo*.

In summary, PRL-3 promotes CRC cell invasion and metastasis by activating MAPK pathways in TAMs to initiate EMT, and PRL-3 may promote angiogenesis by activating the NF-κB pathway in CRC cells.

Acknowledgements

Not applicable.

Funding

The present study was supported by the National Natural Science Foundation of China (no.81871981), the National Natural Science Foundation of Guangdong Province (nos. 2016A030313353 and 2016A030310183), the National Natural Science Foundation of China (nos. 81602539, 81702902 and 81602125) and the Science and Technology Project of Guangdong Province (no. 2015A050502021).

Availability of data and materials

The datasets used and analyzed during the present study are available from the corresponding author on reasonable request.

Authors' contributions

TZ and LL acquired the data after carrying out the experiments, performed the statistical analysis of all experimental results, and created a draft of the manuscript; YZ, HX and PS prepared the experimental materials; WL, QL and ZC revised and approved the final version of the manuscript and were also involved in the conception of the study. All authors read and approved the manuscript and agree to be accountable for all aspects of the research in ensuring that the accuracy or integrity of any part of the work are appropriately investigated and resolved.

Ethics approval and consent to participate

The protocol of the present study was approved by the Institutional Research Ethics Committee of the Sun Yat-Sen Memorial Hospital of Sun Yat-Sen University. All animal protocols were approved by the Institutional Animal Care and Use Committee and Welfare Committee of Sun Yat-Sen University (Guangzhou, China).

Patient consent for publication

Not applicable.

Competing interests

The authors declare that they have no competing interests.

References

1. Sheng N, Yan L, Wu K, You W, Gong J, Hu L, Tan G, Chen H and Wang Z: TRIP13 promotes tumor growth and is associated with poor prognosis in colorectal cancer. Cell Death Dis 9: 402, 2018.
2. Vu T and Datta PK: Regulation of EMT in colorectal cancer: A culprit in metastasis. Cancers 9: E171, 2017.
3. Ferlay J, Soerjomataram I, Dikshit R, Eser S, Mathers C, Rebelo M, Parkin DM, Forman D and Bray F: Cancer incidence and mortality worldwide: Sources, methods and major patterns in GLOBOCAN 2012. Int J Cancer 136: E359-E386, 2015.
4. Lan Q, Lai W, Zeng Y, Liu L, Li S, Jin S, Zhang Y, Luo X, Xu H, Lin X, *et al*: CCL26 participates in the PRL-3-induced promotion of colorectal cancer invasion by stimulating tumor-associated macrophage infiltration. Mol Cancer Ther 17: 276-289, 2018.
5. Xu H, Zhang Y, Peña MM, Pirisi L and Creek KE: Six1 promotes colorectal cancer growth and metastasis by stimulating angiogenesis and recruiting tumor-associated macrophages. Carcinogenesis 38: 281-292, 2017.
6. Ming J, Liu N, Gu Y, Qiu X and Wang EH: PRL-3 facilitates angiogenesis and metastasis by increasing ERK phosphorylation and up-regulating the levels and activities of Rho-A/C in lung cancer. Pathology 41: 118-126, 2009.
7. Liang F, Liang J, Wang WQ, Sun JP, Udho E and Zhang ZY: PRL3 promotes cell invasion and proliferation by down-regulation of Csk leading to Src activation. J Biol Chem 282: 5413-5419, 2007.
8. Guo K, Li J, Wang H, Osato M, Tang JP, Quah SY, Gan BQ and Zeng Q: PRL-3 initiates tumor angiogenesis by recruiting endothelial cells in vitro and in vivo. Cancer Res 66: 9625-9635, 2006.
9. Zimmerman MW, McQueeney KE, Isenberg JS, Pitt BR, Wasserloos KA, Homanics GE and Lazo JS: Protein-tyrosine phosphatase 4A3 (PTP4A3) promotes vascular endothelial growth factor signaling and enables endothelial cell motility. J Biol Chem 289: 5904-5913, 2014.
10. Mager LF, Wasmer MH, Rau TT and Krebs P: Cytokine-induced modulation of colorectal cancer. Front Oncol 6: 96, 2016.
11. Lin X, Yi Z, Diao J, Shao M, Zhao L, Cai H, Fan Q, Yao X and Sun X: ShaoYao decoction ameliorates colitis-associated colorectal cancer by downregulating proinflammatory cytokines and promoting epithelial-mesenchymal transition. J Transl Med 12: 105, 2014.
12. Rokavec M, Öner MG, Li H, Jackstadt R, Jiang L, Lodygin D, Kaller M, Horst D, Ziegler PK, Schwitalla S, *et al*: IL-6R/STAT3/miR-34a feedback loop promotes EMT-mediated colorectal cancer invasion and metastasis. J Clin Invest 125: 1362, 2015.
13. Wang L, Tang C, Cao H, Li K, Pang X, Zhong L, Dang W, Tang H, Huang Y, Wei L, *et al*: Activation of IL-8 via PI3K/Akt-dependent pathway is involved in leptin-mediated epithelial-mesenchymal transition in human breast cancer cells. Cancer Biol Ther 16: 1220-1230, 2015.
14. Xu H, Lai W, Zhang Y, Liu L, Luo X, Zeng Y, Wu H, Lan Q and Chu Z: Tumor-associated macrophage-derived IL-6 and IL-8 enhance invasive activity of LoVo cells induced by PRL-3 in a KCNN4 channel-dependent manner. BMC Cancer 14: 330, 2014.

15. Jedinak A, Dudhgaonkar S and Sliva D: Activated macrophages induce metastatic behavior of colon cancer cells. Immunobiology 215: 242-249, 2010.
16. Erreni M, Mantovani A and Allavena P: Tumor-associated macrophages (TAM) and inflammation in colorectal cancer. Cancer Microenviron 4: 141-154, 2011.
17. Li S, Xu F, Zhang J, Wang L, Zheng Y, Wu X, Wang J, Huang Q and Lai M: Tumor-associated macrophages remodeling EMT and predicting survival in colorectal carcinoma. Oncoimmunology 7: e1380765, 2017.
18. Peng L, Jin G, Wang L, Guo J, Meng L and Shou C: Identification of integrin alpha1 as an interacting protein of protein tyrosine phosphatase PRL-3. Biochem Biophys Res Commun 342: 179-183, 2006.
19. Shi G, Zheng X, Zhang S, Wu X, Yu F, Wang Y and Xing F: Kanglaite inhibits EMT caused by TNF-α via NF-κB inhibition in colorectal cancer cells. Oncotarget 9: 6771-6779, 2017.
20. Zhao WB, Li Y, Liu X, Zhang LY and Wang X: Evaluation of PRL-3 expression, and its correlation with angiogenesis and invasion in hepatocellular carcinoma. Int J Mol Med 22: 187-192, 2008.
21. Sahai E and Marshall CJ: RHO-GTPases and cancer. Nat Rev Cancer 2: 133-142, 2002.
22. Wang H, Quah SY, Dong JM, Manser E, Tang JP and Zeng Q: PRL-3 down-regulates PTEN expression and signals through PI3K to promote epithelial-mesenchymal transition. Cancer Res 67: 2922-2926, 2007.